

Performance simulation of solar-boosted ocean thermal energy conversion plant

Noboru Yamada^{a,*}, Akira Hoshi^b, Yasuyuki Ikegami^c

^a Graduate School of Energy and Environment Science, Nagaoka University of Technology, 1603-1 Kamitomioka, Nagaoka, Niigata 940-2188, Japan

^b Department of Mechanical Engineering, Ichinoseki National College of Technology, Takanashi, Hagisho, Ichinoseki 021-8511, Japan

^c Institute of Ocean Energy, Saga University, Honjo, Saga 840-8502, Japan

ARTICLE INFO

Article history:

Received 14 July 2008

Accepted 28 December 2008

Available online 30 January 2009

Keywords:

Solar thermal energy

Ocean thermal energy conversion

Solar collector

First-order simulation

ABSTRACT

Ocean thermal energy conversion (OTEC) is a power generation method that utilizes small temperature difference between the warm surface water and cold deep water of the ocean. This paper describes the performance simulation results of an OTEC plant that utilizes not only ocean thermal energy but also solar thermal energy as a heat source. This power generation system was termed SOTEC (solar-boosted ocean thermal energy conversion). In SOTEC, the temperature of warm sea water was boosted by using a typical low-cost solar thermal collector. In order to estimate the potential thermal efficiency and required effective area of a solar collector for a 100-kWe SOTEC plant, first-order modeling and simulation were carried out under the ambient conditions at Kumejima Island in southern part of Japan. The results show that the proposed SOTEC plant can potentially enhance the annual mean net thermal efficiency up to a value that is approximately 1.5 times higher than that of the conventional OTEC plant if a single-glazed flat-plate solar collector of 5000-m² effective area is installed to boost the temperature of warm sea water by 20 K.

© 2009 Elsevier Ltd. All rights reserved.

1. Introduction

Ocean thermal energy conversion (OTEC) is a power generation method wherein the heat energy associated with the temperature difference between the warm surface water and cold deep water of the ocean is converted into electricity [1–4]. Considerable research effort has been directed to the development of OTEC. Uehara [5–8] conducted numerous theoretical and experimental studies on the major components of an OTEC plant. The results of these studies revealed that ammonia is one of the suitable working fluids for a closed-Rankine-cycle OTEC plant. However, due to a small temperature difference (approximately 15–25 K) between the surface water and deep water of the ocean, the Rankine-cycle efficiency is limited to be only 3–5%. This results in a high cost of the electricity generated by an OTEC plant. In order to improve the cycle efficiency, other thermodynamic cycles such as Kalina cycle and Uehara cycle that use an ammonia–water mixture as the working fluid have been developed and reported to have better thermal efficiency than the Rankine cycle at the same temperature

difference. However, it is evident that increasing the temperature difference between the hot and cold heat sources is the most effective solution to improve the thermal efficiency of a thermodynamic power generation cycle. Saitoh and Yamada [9] have described a conceptual design of the multiple Rankine-cycle system using both solar-thermal energy and ocean thermal energy in order to improve the cycle efficiency. This concept is quite reasonable because good seasonal solar radiation would be expected at many OTEC candidate sites. Further, in order to reduce material cost and attain low electricity cost, Straatman and Van Sark [10] have reported the conceptual description of a unique OTEC system combined with an offshore solar pond called the OTEC-OSP hybrid system. We consider that the combination of OTEC and typical low-cost solar collectors could be another possible way to improve the cycle efficiency and to attain low-electricity cost.

In this study, we describe a first-order simulation model of the OTEC system that utilizes not only ocean thermal energy but also solar-thermal energy; the latter is used as a secondary heat source. A solar collector used in a residential application is simply installed to the conventional OTEC component. This power generation system is termed as SOTEC (Solar-boosted Ocean Thermal Energy Conversion). The performance simulation of a 100-kWe SOTEC plant with three typical low-cost solar-thermal collectors, which

* Corresponding author. Tel./fax: +81 258 47 9724.

E-mail address: noboru@mech.nagaokaut.ac.jp (N. Yamada).

increase the turbine inlet temperature of the working fluid, is carried out under the actual weather and sea-water conditions at Kumejima Island in the southern part of Japan. The simulation results of the SOTEC plant are discussed and compared with that of the conventional OTEC plant.

2. Simulation model of SOTEC plant

Figs. 1 and 2 show schematics of the conventional closed-Rankine-cycle OTEC operation and the proposed SOTEC operation, respectively; these figures show the general arrangement of the heat exchangers, pumps, piping, turbine generator, and solar collector. In SOTEC, we present two probable ways to install solar collector into the cycle, as shown in Fig. 2(a) and (b). In Fig. 2(a), the warm sea water is pumped from the ocean surface and is heated by a solar collector; then, the working fluid is indirectly heated and evaporated through the evaporator. On the other hand, in Fig. 2(b), the working fluid is directly heated and evaporated by a solar collector after the working fluid is pre-heated by the warm sea water through the heat exchanger. In this study, the former ‘indirect’ SOTEC in Fig. 2(a) was selected for the performance simulation because of some advantages in feasibility over the latter ‘direct’ SOTEC shown in Fig. 2(b). The solar collector in Fig. 2(b) must be prepared to have corrosion resistance and high-pressure tightness to directly heat the ammonia, the working fluid. A large amount of ammonia would be necessary to fill up the entire solar-collector piping in operation. This might increase the operational cost. Moreover, in the case of this direct SOTEC plant, there are safety and security concerns: due care must be exercised in order to prevent the ammonia from leaking into the environment during long-term operation. In addition, for faithful simulation of this plant, we must know the characteristics of the solar collector when it functions as an evaporator and/or a superheating device. For these reasons, in this study, we modeled and simulated the indirect SOTEC. Further, the OTEC of this SOTEC plant is selectively operated in night-time, i.e. in the absence of solar radiation, and even in those times during a day when the solar radiation is insufficient for the SOTEC operation.

In the simulation, an ideal saturated Rankine cycle was assumed in order to determine the theoretical thermal efficiency of the Rankine-cycle η_{th} . Fig. 3 shows the corresponding temperature–ent

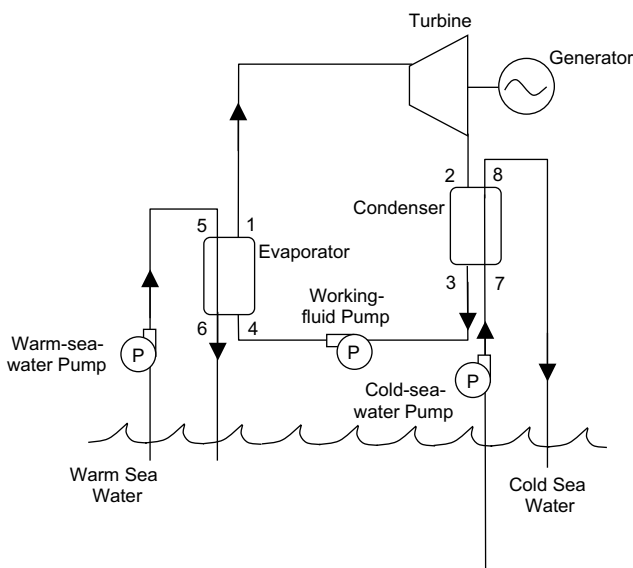


Fig. 1. Schematics of conventional closed-Rankine-cycle OTEC operation.

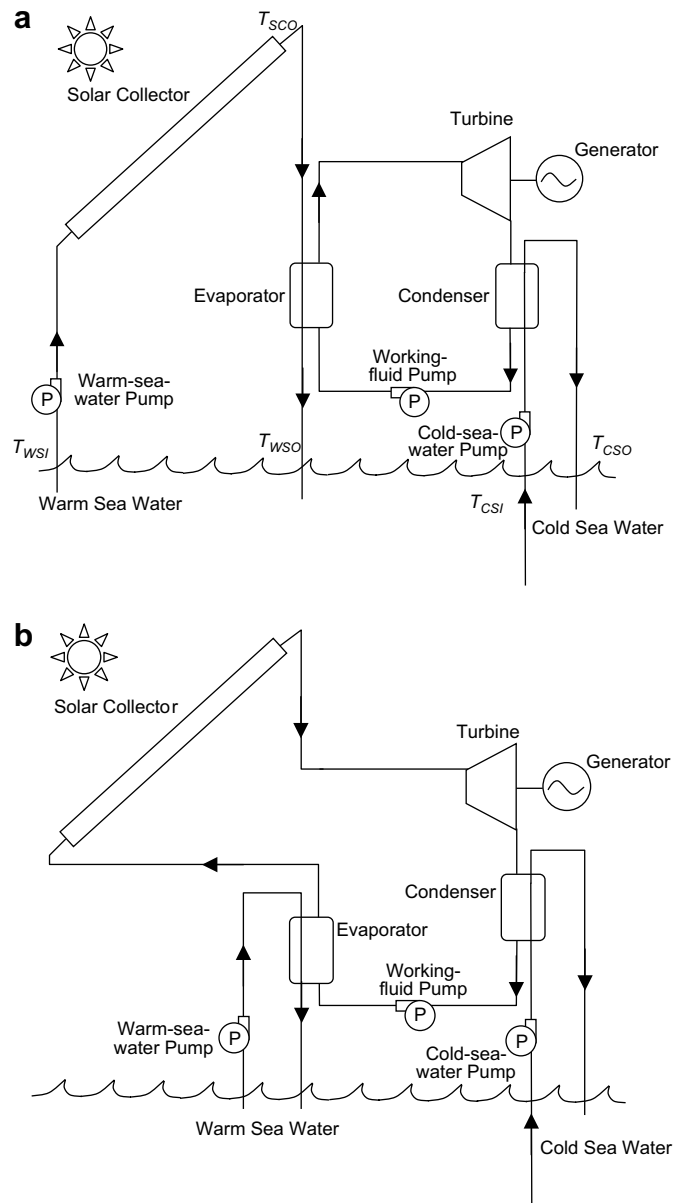


Fig. 2. Schematics of SOTEC operation: (a) Solar collector installed in warm-sea-water line (b) Solar collector installed in working-fluid line.

ropy (T - s) diagram. Here, T_E , T_C , and T_{SCO} are the evaporation temperature, condensation temperature, and the outlet temperature of the solar collector, respectively; T_{WSI} and T_{WSO} , the inlet and outlet temperatures of the warm sea water, respectively; T_{CSI} and T_{CSO} , the inlet and outlet temperatures of the cold sea water, respectively; and Q_E and Q_C , the heat-flow rate at the evaporator and condenser, respectively.

Fig. 4 shows the relationship between the theoretical thermal efficiency of the Rankine-cycle η_{th} and the temperature difference $\Delta T = T_E - T_C$. The conventional OTEC has ΔT between 15 K and 25 K; as a result, the maximum theoretical thermal efficiency is approximately $\eta_{th} = 8\%$. If a solar collector can additionally boost T_E by 20 K, the theoretical thermal efficiency of the SOTEC can be improved up to $\eta_{th} = 13\%$. Pumping power was not considered in the calculation of η_{th} . According to Rafferty [11] and Vega [12], ΔT is the key factor that determines the cost of a solar-thermal energy (STE) plant in the range of low ΔT values due to a logarithmic

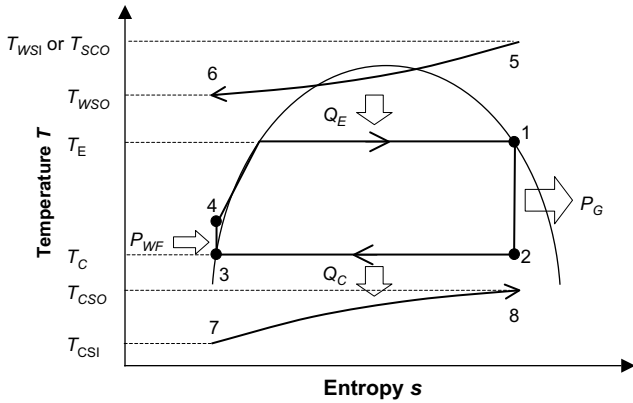


Fig. 3. T-s diagram of the closed-Rankine-cycle; the numbers and variables correspond to Figs. 1 and 2(a).

decrease in the cost with an increase in ΔT . In general, the cost of an STE plant can be significantly reduced by increasing ΔT by 50–80 K from the low-temperature range ($\Delta T=20$ K) to a lower-middle temperature range ($\Delta T=70$ –100 K). However, for SOTEC, we believe that the solar boost of 20–40 K would be preferable because it is difficult to maintain high-thermal efficiency simultaneously in two very different temperature ranges that are associated with daytime SOTEC operation and night-time OTEC operation. Further, using a single working fluid that is reasonably matched with the temperature range associated with OTEC operation would be a cost-effective way.

Fig. 5 shows the collector efficiency curves of a typical single-glazed flat-plate solar collector, evacuated-tube solar collector, and compound-parabolic-concentrator (CPC) solar collector. The efficiency curves were measured by each manufacturer. These collectors are frequently used for residential water-heating applications. Since these collectors are mass-produced, they are cheaper than high-temperature solar concentrating collectors. Therefore, we expect that the installation of these collectors would be cost-effective if the temperature range is less than 60 °C (333.15 K) and the effective collector area is within a certain limit. As shown in Fig. 5, the annual mean collector efficiencies of these solar collectors were estimated to be as high as approximately 65–75% for the weather condition in Kumejima Island (Lat. 26–20N, Lng. 126–48E) near Okinawa Island in Japan, which is the planned construction site of the OTEC plant. Fig. 6 shows the monthly variation of the

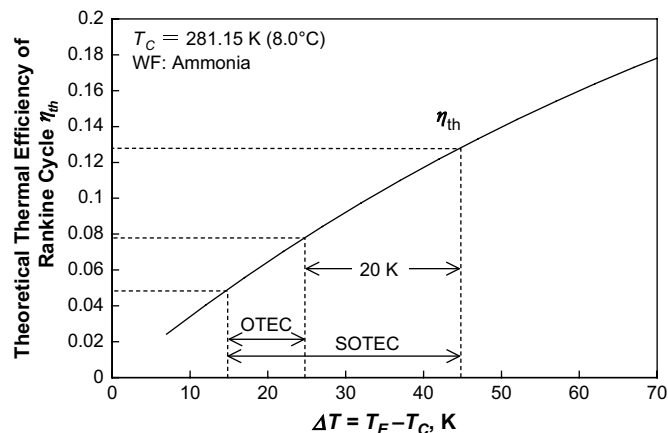


Fig. 4. Relationship between theoretical thermal efficiency of saturated Rankine cycle η_{th} and the operating temperature range ΔT of OTEC and SOTEC.

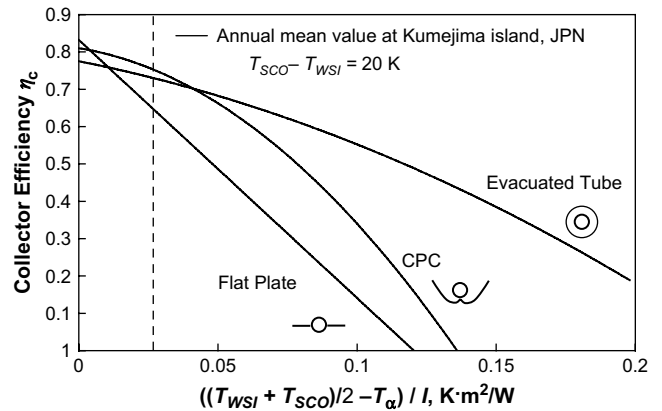


Fig. 5. Collector efficiency of flat-plate, evacuated-tube, and CPC solar collectors.

ambient temperature, the temperatures of the warm sea surface water and cold sea water, and the mean daytime solar radiation to a tilted solar-collector aperture at Kumejima Island [13]. Tilt angle of solar collector is 30° facing the equator. During daytime, from June to October, approximately more than 450 W/m² of solar radiation is available to boost the warm sea-water temperature. In this study, first, for each solar collector, we simulated its effective area that is required for boosting the temperature of warm sea water by 20 K or 40 K in order to achieve a 100-kWe of turbine generator power under the conditions shown for monthly daytime weather and sea-water temperature. Next, we simulated annual hourly performance using these effective areas of the solar collectors.

The following assumptions were applied to the present simulation.

1. The solar-collector efficiency η_c is calculated from the collector efficiency curve shown in Fig. 5. Here, average sea-water temperature inside a solar collector is defined as $(T_{WSI} + T_{SCO})/2$.
2. The thermodynamic cycle of both OTEC and SOTEC is an ideal saturated Rankine cycle using pure ammonia as the working fluid. Turbine efficiency and pump efficiency are given explicitly.
3. The heat losses from piping and other auxiliary components are negligible.

The net power P_N of the OTEC or SOTEC operation is defined as

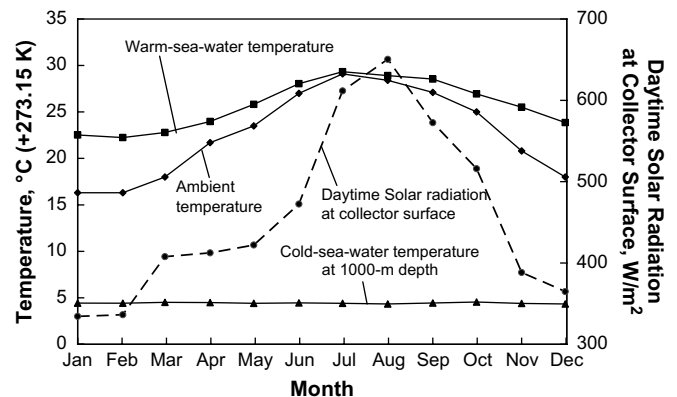


Fig. 6. Monthly variation of ambient temperature, the temperatures of the warm sea surface water and cold sea water, and mean solar-radiation incident on a tilted solar-collector surface at Kumejima island in Japan.

$$P_N = P_G - (P_{WS} + P_{CS} + P_{WF}) \quad (1)$$

where P_G is the turbine generator power and P_{WS} , P_{CS} , and P_{WF} are the pumping powers required for warm sea water, cold sea water, and the working fluid, respectively. Generally, a power generation cycle that employs a low-temperature difference tends to consume larger pumping electricity than the one that employs a high-temperature difference. Therefore, it is important to simulate net power and net thermal efficiency in OTEC and SOTEC. The value of P_G is calculated as follows from the product of the mass flow rate of the working-fluid m_{WF} and the adiabatic enthalpy difference between the evaporator and the condenser:

$$P_G = m_{WF} \eta_T \eta_G (h_1 - h_2) \quad (2)$$

where η_T and η_G are the turbine and generator efficiencies, respectively. The values of enthalpies h_1 and h_2 are calculated using PROPATH [14] (Stewart et al. [15]), software for calculating thermodynamic properties. The values of P_{WS} , P_{CS} , and P_{WF} are calculated as follows:

$$P_{WS} = m_{WS} \Delta H_{WSg} / \eta_{WSP} \quad (3)$$

$$P_{CS} = m_{CS} \Delta H_{CSg} / \eta_{CSP} \quad (4)$$

$$P_{WF} = m_{WF} \Delta H_{WFG} / \eta_{WFP} \quad (5)$$

where g is the acceleration due to gravity and m_{WS} , m_{CS} , m_{WF} , ΔH_{WS} , ΔH_{CS} , ΔH_{WF} , η_{WSP} , η_{CSP} , and η_{WFP} are mass flow rate, total pressure difference (i.e. head), and pump efficiency of the piping used for warm sea water, cold sea water, and working fluid, respectively. The pressure difference of each piping was calculated using the equations derived by Uehara and Ikegami [6]. They have performed a detailed optimization of a closed-Rankine-cycle 1-MWe OTEC plant with plate-type heat exchangers using ammonia as the working fluid. Fig. 7 shows a piping diagram of the proposed SOTEC plant. Its operation was alternatively switched from OTEC to SOTEC by controlling valves. The heat transfer areas of the evaporator and condenser were also ideally controlled to the optimal heat exchange efficiency by controlling valves. Table 1 shows the piping condition of the 100-kWe SOTEC plant. The specification of the plate-type heat exchanger was the same as that reported by Uehara

and Ikegami [6]. The total pressure head of the solar-collector array including piping and auxiliary was assumed to be 15 m.

Table 2 shows the other conditions for the simulation. The overall heat transfer coefficients of the evaporator U_E and the condenser U_C were assumed to be 4000 W/m²K and 3500 W/m²K, respectively. These values have been experimentally obtained by Uehara and Nakaoka [5]. The heat transfer areas of the evaporator A_E and the condenser A_C are defined as

$$A_E = Q_E / (U_E (\Delta T_m)_E) = m_{WS} c_{pWS} (T_{WSI} - T_{WSO}) / (U_E (\Delta T_m)_E) \quad (6)$$

$$A_C = Q_C / (U_C (\Delta T_m)_C) = m_{CS} c_{pCS} (T_{CSO} - T_{CSI}) / (U_C (\Delta T_m)_C) \quad (7)$$

where, $(\Delta T_m)_E$ and $(\Delta T_m)_C$ are the logarithmic mean temperature differences of the evaporator and the condenser, respectively. Q_E and Q_C are the heat flow rate of the evaporator and the condenser, respectively, defined as

$$Q_E = m_{WF} (h_1 - h_4) \quad (8)$$

$$Q_C = m_{WF} (h_2 - h_3) \quad (9)$$

The Rankine-cycle efficiency η_R and the net Rankine-cycle efficiency η_{net} are given as follows:

$$\eta_R = P_G / Q_E \quad (10)$$

$$\eta_{net} = P_N / Q_E \quad (11)$$

3. Results and discussion

First, the conventional 100-kWe OTEC operation was simulated and the heat transfer areas of the evaporator and condenser were determined in advance, the SOTEC daytime operation was then simulated by optimizing the flow rates of warm and cold sea water in order to avoid the required heat transfer capacities of the evaporator and condenser from exceeding the determined values for the OTEC operation: $A_E = 514 \text{ m}^2$ and $A_C = 478 \text{ m}^2$. In SOTEC, the increase in the turbine inlet temperature, i.e. the increase in the evaporation temperature caused by the solar boost is assumed to be

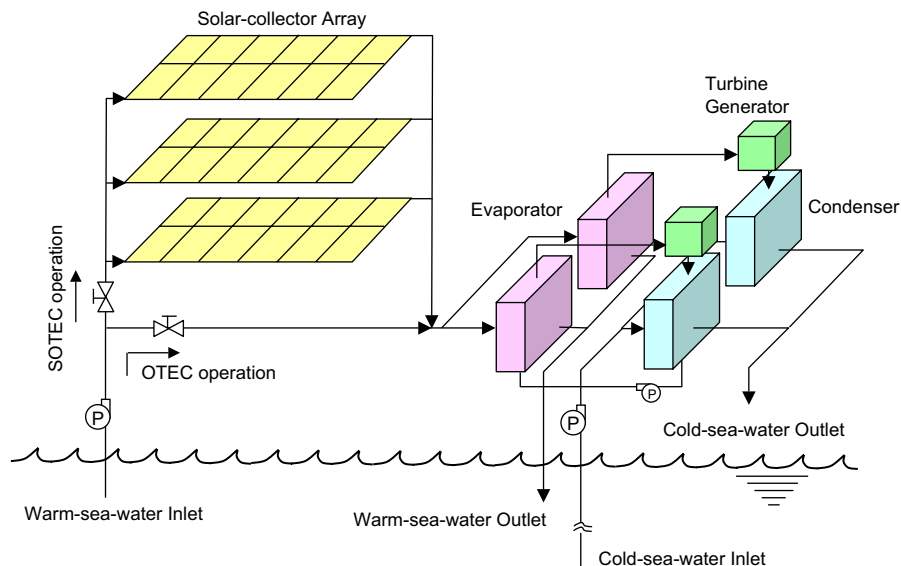


Fig. 7. Piping diagram of the SOTEC plant.

Table 1
Piping conditions for the simulation.

Warm-sea-water pipe			
Length	m	50	
Diameter	m	0.7	
Cold-sea-water pipe			
Length	m	1000	
Diameter	m	0.7	
Plate-type heat exchanger (as evaporator and condenser)			
Plate length	m	4.0	
Plate width	m	1.5	
Plate thickness	mm	1.0	
Clearance on sea water side	mm	5.0	
Clearance on working-fluid side	mm	5.0	
Total pressure head of solar-collector array and piping	m	15	

20 K, and the solar-collector areas required for achieving the 20-K solar boost were estimated.

Fig. 8 shows the monthly variation of the daytime net Rankine-cycle efficiency η_{net} of SOTEC operation compared with that of OTEC operation. η_{net} of SOTEC is approximately three times higher than that of OTEC in every month. This improvement was better than we expected in the preliminary consideration of the theoretical thermal efficiency η_{th} , as shown in Fig. 4. η_{net} of SOTEC was significantly affected by pumping powers.

Fig. 9 shows the monthly variations of the net power P_N and the pumping powers required for warm-sea-water P_{WS} , cold-sea-water P_{CS} , and the working-fluid P_{WF} : Fig. 9(a) and (b) is for OTEC and SOTEC operations, respectively. These figures show a breakdown of turbine-generated power $P_G = 100$ kW. In SOTEC operation, the pumping power required for cold sea water was reduced to approximately 30% of that in OTEC operation because the mass flow rate of cold sea water was reduced in SOTEC operation due to an increase in the Rankine-cycle efficiency η_R by solar boosting. Consequently, the net power of SOTEC was larger than that of OTEC. The pumping powers required for warm sea water and the working fluid were also slightly reduced in SOTEC. These resulted in the above-mentioned increase in the net efficiency of SOTEC. We should note that the night-time performance of OTEC is almost the

Table 2
Conditions for monthly simulation.

Turbine generator power	P_G	kWe	100
Turbine efficiency	η_T	–	0.80
Generator efficiency	η_G	–	0.90
Efficiency of sea water pump	η_{WSP}	–	0.80
	η_{CSP}	–	0.80
Efficiency of working-fluid pump	η_{WFP}	–	0.75
Evaporator (plate-type heat exchanger)			
Overall heat transfer coefficient	U_E	W/m ² K	4000
$T_{WSI} - T_E$ (OTEC) and $T_{SCO} - T_E$ (SOTEC)		K	3.0
Condenser (plate-type heat exchanger)			
Overall heat transfer coefficient	U_C	W/m ² K	3500
$T_C - T_{CSI}$		K	3.0
Solar collector			
Tilt angle	°		30
Azimuth angle	°		0 (facing South)
Weather condition (Annual mean value in Kumejima, Japan)			
Ambient temperature	T_a	°C	22.6
Solar radiation on collector surface	I	W/m ²	457
Sea water temperature (Annual mean value in Kumejima, Japan)			
Warm-sea-water temperature at a depth of 0 m	°C		25.7
Cold-sea-water temperature at a depth of 1000 m	°C		4.4

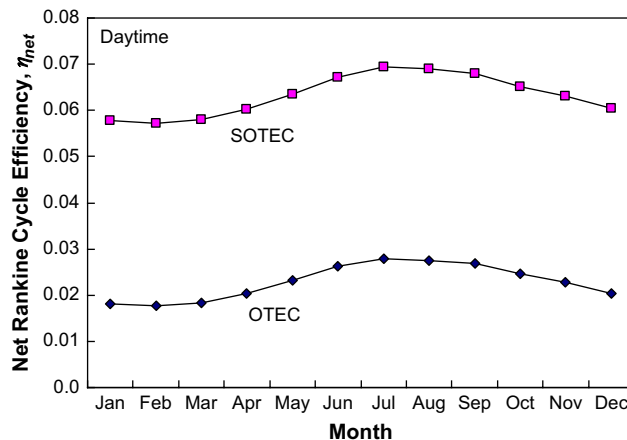


Fig. 8. Monthly variation of daytime net Rankine-cycle efficiency η_{net} of OTEC and SOTEC operation at Kumejima island.

same as the daytime performance since the temperature difference between the warm and cold sea water almost remains the same.

Fig. 10 shows the effective area of a solar-collector A_{SC} required for achieving the 20-K solar boost in monthly 100-kWe SOTEC operation. A_{SC} of the flat-plate collector varied from 4200 m² to 5000 m², while those of the evacuated-tube and CPC collectors varied from 3500 m² to 4500 m². In the summer months, the effective area of the flat-plate collector was more by a maximum of 800 m² than that of the other collectors because the efficiency of this collector decreased with the increase in the temperature of warm sea water, i.e. with the increase in the inlet temperature of this collector in summer months.

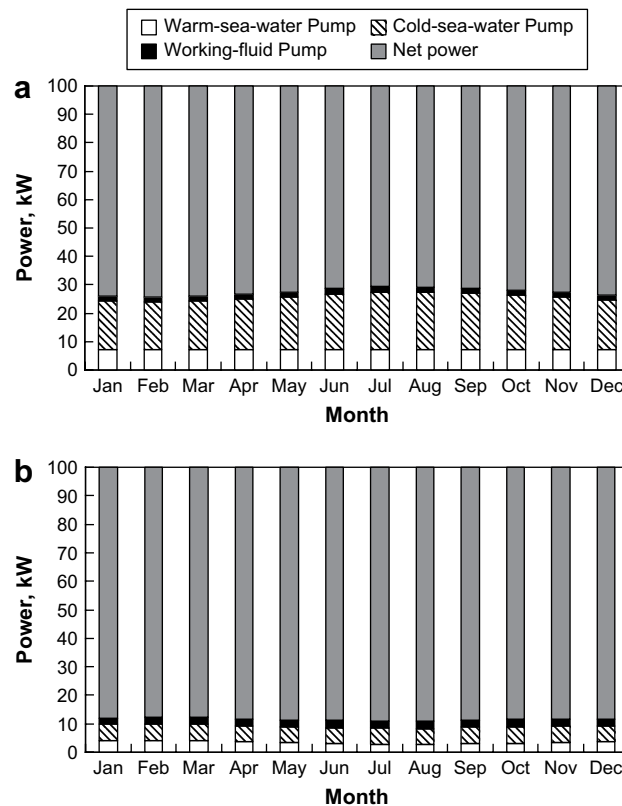


Fig. 9. Monthly variation of net power P_N , warm-sea-water pumping power P_{WS} , cold-sea-water pumping power P_{CS} and working-fluid pumping power P_{WF} in daytime operation at Kumejima island: (a) OTEC operation (b) SOTEC operation.

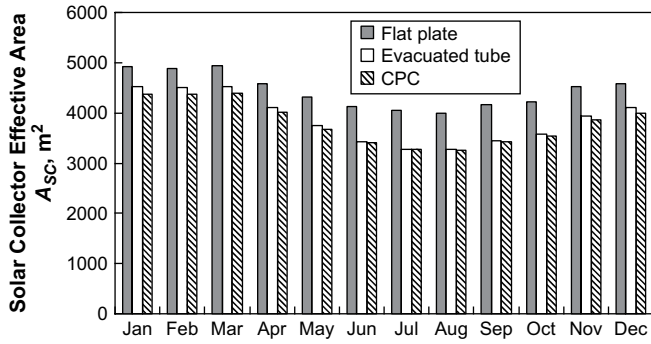


Fig. 10. Required effective area A_{sc} of solar collector for achieving temperature increase of 20 K in 100-kWe SOTEC operation at Kumejima island.

Table 3 lists important simulated values of 100-kWe OTEC and SOTEC operations under the annual mean daytime condition at Kumejima Island. In this table, the result obtained for the case of 40-K solar boost is added for comparison. η_{net} of OTEC daytime operation was 2.3%, while that of SOTEC was 6.3% and

Table 3
Simulation results of 100-kWe OTEC and SOTEC operation under the conditions of annual mean daytime ambient temperature, solar radiation, and sea-water temperature at Kumejima island in Japan.

		OTEC	SOTEC	SOTEC	
			$T_{SCO} - T_{WSI} = 20$ K	$T_{SCO} - T_{WSI} = 40$ K	
Warm sea water:					
inlet temperature	T_{WSI} °C	25.7	25.7	25.7	
Outlet temperature	T_{WSO} °C	22.6	22.8	31.5	
Cold sea water:					
inlet temperature	T_{CSI} °C	4.4	4.4	4.4	
Outlet temperature	T_{CSO} °C	7.4	8.5	8.5	
Solar collector:					
inlet temperature	T_{SCI} °C	–	25.7	25.7	
Outlet temperature	T_{SCO} °C	–	45.7	65.7	
Evaporation temperature	T_E °C	21.7	41.7	61.7	
Condensate temperature	T_C °C	8.4	8.4	8.4	
Net power		P_N kW	72.5	88.4	91.3
Pumping power for:		P_{WS} kW	7.1	3.4	1.5
warm sea water					
Cold sea water	P_{CS} kW	18.6	5.7	3.7	
Working fluid	P_{WF} kW	1.8	2.5	3.5	
Flow rate: warm sea water		m_{WS} kg/s	260	16.0	7.3
Cold sea water	m_{CS} kg/s	260	81.2	52.4	
Working fluid	m_{WF} kg/s	2.6	1.1	0.76	
Rankine-cycle efficiency		η_R %	3.2	7.2	10.4
Net Rankine-cycle-efficiency		η_{net} %	2.3	6.3	9.5
Heat transfer area of evaporator		A_E m ²	514	237	166
Heat transfer area of condenser		A_C m ²	478	299	207
Flat-plate solar collector					
Collector efficiency	η_c –	–	0.63	0.48	
Required collector effective area	A_{sc} m ²	–	4440	5333	
Evacuated-tube collector					
Collector efficiency	η_c –	–	0.73	0.68	
Required collector effective area	A_{sc} m ²	–	3874	3760	
CPC solar collector					
Collector efficiency	η_c –	–	0.74	0.65	
Required collector effective area	A_{sc} m ²	–	3798	3945	

Note: Temperature unit °C is converted into K by adding 273.15 to its value.

9.5% corresponding to 20-K and 40-K solar boost, respectively. The effective area A_{sc} of the flat-plate solar collector for the 40-K solar boost is 5333 m², which is 893 m² larger than that of the 20-K solar boost because of the collector efficiency drop from $\eta_c = 63\%$ to 48%. In contrast, A_{sc} of the evacuated-tube collector for the 40-K solar boost is approximately 100 m² less than that for the 20-K solar boost because the collector efficiency was retained at $\eta_c = 68\%$ even for the 40-K boost.

Fig. 11 shows the simulation results for the annual hourly variation of the net Rankine-cycle efficiency η_{net} of the SOTEC plant and the conventional OTEC plant at Kumejima Island for the 20-K solar boost. In this simulation, we used a transient system simulation program TRNSYS ver. 15. We selected a flat-plate single-glazed solar collector, called TYPE1 collector, with an effective area of 5000 m². We originally developed closed-Rankine-cycle module, which switches OTEC and SOTEC operation and controls mass flow rates to maintain the optimal Rankine-cycle efficiency. The evaporation and condensation temperatures were calculated from energy balances in accordance with the manner described by Morrison [16]. The piping and other conditions were the same as those listed in Tables 1 and 2, respectively. The annual mean values of hourly solar radiation and ambient temperature were inputted, while the monthly mean values of sea water temperatures were inputted since the daily variation in the sea water temperature is insignificant. The SOTEC plant was selectively operated in the SOTEC mode during daytime only if the thermal efficiency of SOTEC operation exceeded that of OTEC operation. In Fig. 11, η_{net} of the SOTEC plant fluctuated up to 9% due to the change in solar gain, while η_{net} of OTEC was within the range between approximately 1% and 3%. Further, the net power of SOTEC fluctuated within the range between approximately 70 kWe and 150 kWe; this is not shown in Fig. 11. The annual total SOTEC operation time at Kumejima Island was estimated to be 2867 h (approximately 120 days), so that the annual mean net Rankine-cycle efficiency of the SOTEC plant was finally estimated to be approximately 3%. This value is equivalent to 145% of that of the conventional OTEC plant.

The present simulation results indicate that the SOTEC operation can potentially increase the efficiency of OTEC by means of a combination of low-cost solar collectors. 40-K boost by the solar collector enhances net thermal efficiency up to several times higher than the conventional OTEC in daytime. This performance enhancement is a comparable level to that of OTEC-OSP (a hybrid OTEC combined with offshore solar pond) estimated by Straatman and Van Sark [10]. We expect that SOTEC can be one of the designs such that has an economically optimal efficiency as well as OTEC-OSP. However, in terms of cost estimation for the SOTEC, more

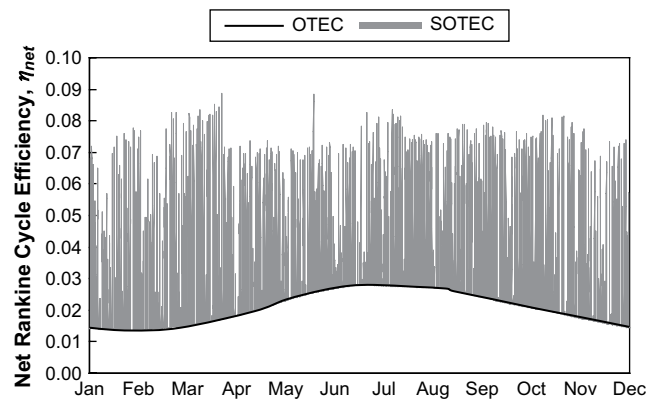


Fig. 11. Hourly variation of net Rankine-cycle efficiency η_{net} of SOTEC plant and conventional OTEC plant at Kumejima island in case of temperature increase of 20 K by flat-plate solar collector with effective area of 5000 m².

careful consideration and analysis of electricity cost is necessary along with practical construction planning. At this moment, we would like to emphasize that the cost of a flat-plate solar collector would be lower than that of other solar collectors if we aim to achieve a solar boost of within 20 K and that the evacuated-tube collector would be cost-effective for the SOTEC with 40-K solar boost. The price of evacuated-tube collectors is being dramatically reduced due to market expansion and the development of mass-production technology. The development of a mass-production technology for large-area solar collectors will help reduce the cost of SOTEC. For collector-mounting cost, in tropical sunny-island nations around the equator where OTEC potentially works most efficiently, it is obvious that the solar collectors need not be tilted for receiving the best solar-radiation gain. This implies that one can construct a solar-collector array on the sea surface with a floating raft or on the flat beach with less mounting materials. However, particular plumbing piping and sealing might be required for the collector and auxiliaries in order to prevent the damage from salt water and waves. These costs should be carefully estimated in order to judge the practical feasibility and reliability of an SOTEC plant. Furthermore, we should consider that there are other thermodynamic cycles that are more efficient and advanced than the closed-Rankine-cycle used in the present simulation. More precise performance simulation based on these other efficient cycles is necessary.

4. Conclusion

A solar-boosted ocean thermal energy conversion (SOTEC) system was proposed and first-order performance simulation was carried out. The results reveal that the installation of a solar collector enhances the thermal efficiency of an OTEC plant, particularly in daytime operation. Net thermal efficiency of SOTEC operation with 20-K solar boost is 2.7 times higher than that of OTEC operation under the daytime conditions at Kumejima Island. This results in approximately 1.5-times higher annual net thermal efficiency than the conventional OTEC plant. For future studies, the authors intend to perform more precise simulation including other thermodynamic cycles and estimate the practical cost of SOTEC plant. We believe that the direct SOTEC system shown in Fig. 2(b) would be worth considering in addition to the indirect SOTEC system focused in this paper. We will experimentally verify the efficiency enhancement by installing a solar collector into the 30-kW OTEC test plant which has already been constructed and operated at Institute of Ocean Energy, Saga University [17,18]. The development of an advanced OTEC system will become increasingly important and promising with a long-term upward trend in the prices of oil and fossil fuels.

Acknowledgments

This study was conducted under the Cooperative Research Program of the Institute of Ocean energy, Saga University (Research No.05001A). N. Yamada thanks Dr. Graham L. Morrison, Emeritus Professor of University of New South Wales for his valuable assistance for the TRNSYS simulation and Dr. Takeo S. Saitoh, Emeritus Professor of Tohoku University, for his valuable support.

References

- [1] Avery WH, Wu C. Renewable energy from the ocean—A guide to OTEC. Oxford: Oxford University Press; 1994.
- [2] Dylan T. Ocean thermal energy conversion: current overview and future outlook. *Renewable Energy* 1995;6(3):367–73.
- [3] Cavrot DE. Economics of ocean thermal energy conversion (OTEC). *Renewable Energy* 1993;3(8):891–6.
- [4] Lennard DE. The viability and best locations for ocean thermal energy conversion systems around the world. *Renewable Energy, World renewable energy congress climate change. Energy and the Environment* 1995;6(3): 359–65.
- [5] Uehara H, Nakaoka T. OTEC using plate-type heat exchanger (using ammonia as working fluid). *Transactions of JSME* 1984;50(453):1325–33 [in Japanese].
- [6] Uehara H, Ikegami Y. Optimization of a closed-cycle OTEC system. *Journal of Solar Energy Engineering, Transactions of ASME* 1990;112:247–56.
- [7] Uehara H, Miyara A, Ikegami Y, Nakaoka T. Performance analysis of an OTEC plant and a desalination plant using an integrated hybrid cycle. *Journal of Solar Energy Engineering, Transactions of ASME* 1996;118:115–22.
- [8] Uehara H, Dilao CO, Nakaoka T. Conceptual design of ocean thermal energy conversion power plants in the Philippines. *Solar Energy* 1998;41(5):431–41.
- [9] Saitoh TS, Yamada N. Advanced multiple Rankine cycle system including Uehara cycle for solar and ocean energy utilization. In: *Proceedings of forum on desalination using renewable energy*; 2003. p.167–75.
- [10] Straatman Paul JT, van Sark Wilfried GJHM. A new hybrid ocean thermal energy conversion-offshore solar pond (OTEC-OSP) design: a cost optimization approach. *Solar Energy* 2008;82(6):520–7.
- [11] Rafferty K. Geothermal power generation, a primer on low temperature small scale applications, geo-heat center. Available from: . Klamath Falls, OR: Oregon Institute of Technology <<http://geoheat.oit.edu/pdf/powergen.pdf>>; 2000.
- [12] Vega LA. Renewable ocean energy – an overview of the state of the art. *Marine Technology Society Journal* 2002/2003;36:25–35.
- [13] Architectural institute of Japan. Expanded AMeDAS weather data. Architectural Institute of Japan; 2000.
- [14] PROPATH. A program package for thermophysical properties, version 12.1. PROPATH Group; 2001.
- [15] Stewart RB, Jacobsen RT, Renoncello SG. ASHRAE thermodynamic properties of refrigerants, vol. 93–7. American Society of Heating, Refrigerating and Air-Conditioning Engineers; 1986. p. 262–282.
- [16] Morrison GL. Simulation of packaged solar heat-pump water heaters. *Solar Energy* 1994;53(3):249–57.
- [17] Yasunaga T, Ikegami Y, Monde M. Performance test of 30 kW OTEC system using ammonia/water as working fluid (effects of heat source temperature and flow rate), vol. 13. OTEC, Institute of Ocean Energy Saga University Japan; 2007. p. 87–94 [in Japanese].
- [18] Yasunaga T, Ikegami Y, Asou H, Monde M. Performance test of 30 kW OTEC system using ammonia/water as working fluid (Effects of composition of ammonia/water mixture). In: OTEC, Institute of Ocean Energy Saga University Japan, vol. 13; 2007. p. 95–102 [in Japanese].